Biosensors and Bioelectronics 167 (2020) 112521

Contents lists available at ScienceDirect

Biosensors and Bioelectronics

journal homepage: http://www.elsevier.com/locate/bios

Batch fabrication of electrochemical sensors on a glycol-modified polyethylene terephthalate-based microfluidic device

Feiyun Cui [a,1], Hamed Jafarishad [b,1], Zhiru Zhou [a], Jiazhang Chen [c], Jiahui Shao [d], Qi Wen [c], Yuxiang Liu [b], H. Susan Zhou [a,*]

[a] Department of Chemical Engineering, Worcester Polytechnic Institute, 100 Institute Road, Worcester, MA, 01609, United States
[b] Department of Mechanical Engineering, Worcester Polytechnic Institute, 100 Institute Road, Worcester, MA, 01609, United States
[c] Department of Physics, Worcester Polytechnic Institute, 100 Institute Road, Worcester, MA, 01609, United States
[d] School of Environmental Science and Engineering, Shanghai Jiao Tong University, 800 Dongchuan Road, Shanghai, 200240, China

ARTICLE INFO

Keywords:
Low-cost electrochemical sensor
Flexible electrochemical sensor
PETG polymer microfluidic device
Dopamine detection

ABSTRACT

Developing low-cost methods for the fabrication of electrochemical microfluidic devices is urgently needed for transferring such devices from fundamental research to daily-life technology. Herein, glycol-modified polyethylene terephthalate (PETG)-based microfluidic devices with embedded channels and gold film electrode (GFE) are developed by a one-step, low-cost, straightforward, and mass-producible method, and are sealed by a reversible hydrophilic tape-based mechanism. Easily accessible poly (methyl methacrylate) (PMMA), polyethylene terephthalate (polyester, PET), and PETG are explored as substrate options for fabricating electrochemical sensors. The results demonstrated that PETG can be an excellent substrate for fabricating the electrode. The electrochemical stability and morphology of the device are investigated. Both redox ions ($[Fe(CN)_6]^{3-/4-}$) and redox organic compounds (dopamine) are used as model analytes to prove the electrochemical performance of the device. The PETG-based microfluidic devices integrated with electrochemical sensors can be used as alternative electrochemical devices for the detection of biological and chemical analytes. Meanwhile, batch-fabricated flexible electrochemical sensors based on PETG film and their electrochemical performance are reported.

1. Introduction

The electrochemical sensor is one of the most popular sensors applied in food safety, environmental monitoring, and biomedical diagnostics (Cui et al., 2020b; Oliveira et al., 2020; Yang et al., 2019). It possesses the advantages of low cost, simplicity, ease of miniaturization, and the ability to be mass fabricated. They also can be used as point-of-care (POC) devices at home or a doctor's office (Cui et al., 2019). Microfluidic devices are designed for handling the analytical procedures with several advantages, such as a short time for analysis, the reduction of reagent costs, and the improvement of repeatability, portability and biocompatibility (Lee et al., 2020; Nikoleli et al., 2018). Combining electrochemical sensors and microfluidic devices is greatly attractive for both chemical and biomedical analytes (Cincotto et al., 2019; da Silva et al., 2019). Hence, great efforts about microfluidic devices integrated with electrochemical sensors are reported (Fava et al., 2019; Fernández-la-Villa et al., 2019; Wang et al., 2019). Usually, the reported electrochemical microfluidic devices are made of silicon or glass substrate and polydimethylsiloxane (PDMS) cover with a special channels (Liu et al., 2018; Wang et al., 2017b). Silicon or glass-based mold is required for patterning the PDMS cover. The fabrication of the mold is a molding process which needs to use photolithography or e-beam lithography, while the sealing of the fluidic channels requires plasma surface treatments. Both the fabrication and sealing processes are time-consuming and require cleanroom equipment.

For these electrochemical microfluidic devices to evolve from fundamental research to accessible everyday technology, developing reasonably less expensive methods for the fabrication of electrochemical microfluidic devices is urgently needed. Polymer microfluidic devices have the merits of easier microfabrication and low cost (Rodrigues et al., 2015). Although extensive research has been carried out on polymer microfluidic devices (Choi and Cunningham, 2006; Jang et al., 2019;

* Corresponding author.
E-mail address: szhou@wpi.edu (H.S. Zhou).
[1] Both authors contributed equally to this work.

https://doi.org/10.1016/j.bios.2020.112521
Received 12 July 2020; Received in revised form 13 August 2020; Accepted 14 August 2020
Available online 18 August 2020

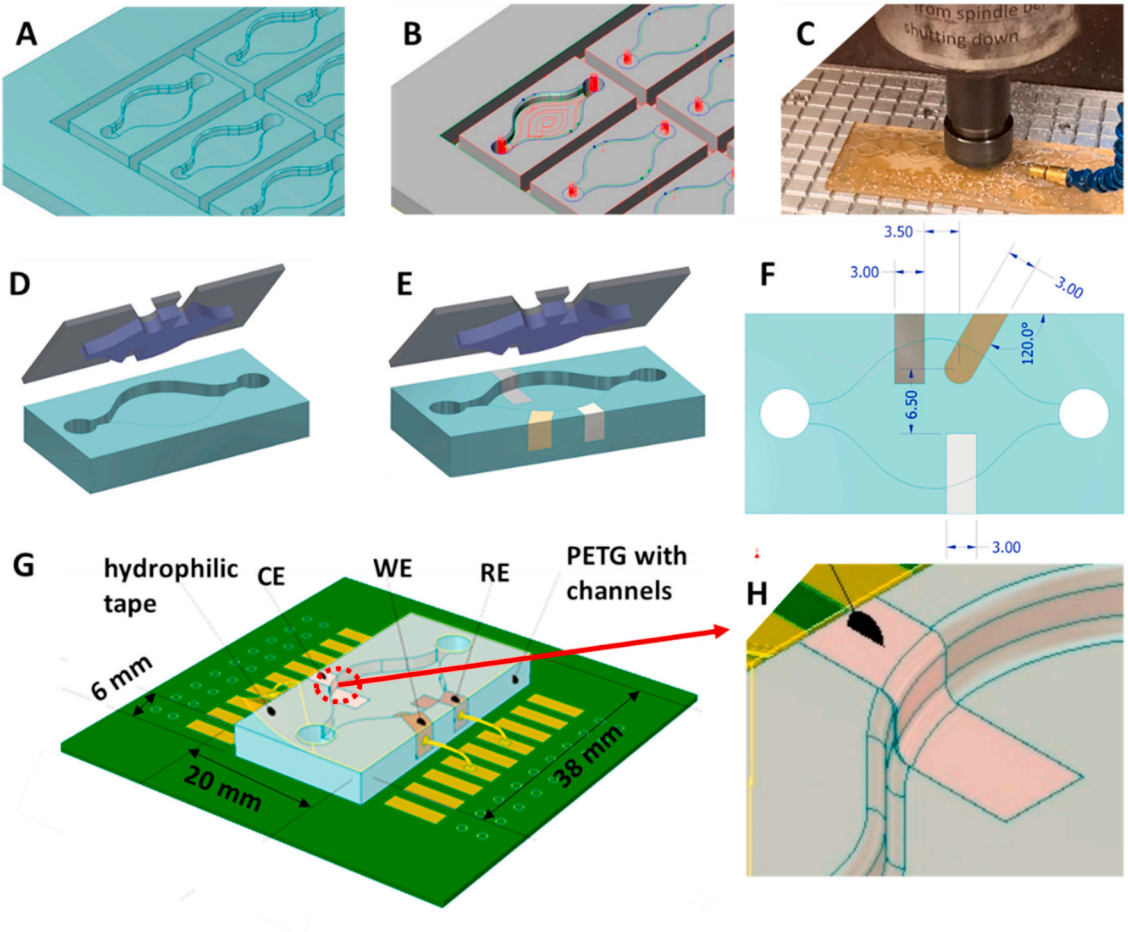

Fig. 1. Schematic diagrams to illustrate the preparation of electrochemical biosensor on the PETG-based microfluidic devices. (A) 3D model of an array of the devices with the desired channels; (B) Generate the corresponding NC codes for the milling process; (C) The devices are patterned by the CNC machine; (D) 3D model of PET-PDMS mask and fit it to the PETG microfluidic device; (E) Remove the PET-PDMS mask from the PETG microfluidic device after sputtering gold or other metal layers. (F) 2D model of the channel and electrodes; (G) View of the whole device with embedded channels, hydrophilic tape as a cover, electrodes and PCB as a connector between electrodes and electrochemical instrument; (H) Enlarged view of electrode connection. (For interpretation of the references to colour in this figure legend, the reader is referred to the Web version of this article.)

Ren et al., 2019; Tsao, 2016), only a few of the research activities integrated an electrochemical sensor to the polymer microfluidic devices. An interdigitated electrode (IDE) array was fabricated on a polyethylenenaphtalate (PEN) substrate to develop an impedimetric biosensor in the polymer microfluidic cartridge (Lakey et al., 2019). Monolithic integration of three-material electrodes for the electrochemical sensor was prepared on poly (methyl methacrylate) (PMMA, also called acrylic) substrates (Liu et al., 2013). However, both of them used photolithography to prepare the electrodes. Batch processing and photolithography-free methods need to be developed. Furthermore, our results demonstrated that PMMA is not ideal for depositing Cr/Au film (Cr film as an adhesive layer) since common tape can easily peel off the Cr/Au film from PMMA. Therefore, a better polymer substrate or polymer microfluidic device for electrodes fabrication should be extensively explored and demonstrated.

In this paper, three polymer substrates including PMMA, polyethylene terephthalate (polyester, PET), and glycol-modified polyethylene terephthalate (PETG) are explored for preparing electrochemical microfluidic devices. A simple and low-cost methodology for the fabrication of PETG-based microfluidic devices with embedded channels and gold film electrode (GFE) is developed. A reversible hydrophilic tape-based sealing mechanism is applied. The morphology, elemental composition and phase structures of the GFE are characterized. Two analytes including redox ions ($[Fe(CN)_6]^{3-/4-}$) and redox organic compounds (dopamine) are employed to prove the electrochemical performance of the device. Meanwhile, batch-fabricated flexible electrochemical sensors based on PETG film are presented.

2. Experiment and methods

2.1. Chemicals and materials

Potassium ferricyanide ($K_3[Fe(CN)_6]$, AR), potassium ferrocyanide ($K_4[Fe(CN)_6]$, AR), potassium chloride (KCl, AR), dopamine (DA), and ascorbic acid (AA) were all purchased from Sigma Aldrich (USA). Poly (methyl methacrylate) (PMMA, acrylic) sheet (thickness 2 mm), polyethylene terephthalate glycol (PETG) sheet (thickness 6 mm), polyethylene terephthalate (polyester, PET) film (thickness 0.5 mm) were purchased from McMaster-Carr (USA). PETG film (thickness 0.5 mm) was purchased from Curbell Plastics, Inc. (USA).

2.2. Preparation of PETG microfluidic device

The microfluidic channels are patterned by computer numerical control (CNC) milling, with the fabrication process briefly described below. First, a 3D model of an array of the devices with the desired channels was prepared using a commercial computer-aided design (CAD) software (SolidWorks, Dassault Systèmes), as shown in Fig. 1A. The 3D model was imported into commercial computer-aided

Table 1
Features comparison between different methods for batch fabrication of EC microfluidic devices.

Substrate	Fabrication method	Features	Ref.
paper (cellulose ester)	fast-drying silver paint	Thin layer diffusion rather than planar diffusion	Wang et al. (2017a)
carbon cloth	purchased	Just including working electrode, fabricated in large scale	Shi et al. (2019)
Ni-G-PLA	3D-printing	Just including working electrode	Rocha et al. (2020)
Kapton (polyimide) sheets	piezo-driven inkjet printed	The prepared EC sensor should be housed in a special microfluidic device	Carvajal et al. (2018)
PET films	screen-printed (slot-die coating within an R2R process)	Large-scale manufacturing, without embedded channels	Cagnani et al. (2020)
PET films	R2R gravure Printed		Bariya et al. (2018)
PETG- sheets	On-step CNC milling and sputtering	With embedded channels and GFE, sealed by a reversible hydrophilic tape-based mechanism	This work

EC: electrochemical. GFE: gold film electrode. Ni-G-PLA: $Ni(OH)_2$ microparticles and graphene within a polylactic acid matrix. PET: poly (ethylene terephthalate). R2R: roll-to-roll. SPCE: screen-printed carbon electrode.

manufacturing (CAM) software (ESPRIT, DP Technology Corp) to generate the corresponding numerical control (NC) codes for the milling process (Fig. 1B). The generated code was uploaded to a CNC machine (TM-1, HAAS Automation, Inc) and the devices are patterned by the CNC machine in a 6-mm-thick PETG sheet. The fabrication process is finished by cutting out the devices from the sheet (Fig. 1C). A 3D PET-PDMS mask (Fig. 1D) was designed and prepared as described in detail in supplemental materials S1. The 3D PET-PDMS mask was fitted into the PETG microfluidic device (Fig. 1D). Subsequently, 10 nm Cr and 100 nm Au films were sputtered on the PETG microfluidic devices using ATC ORION sputtering system (AJA International, Inc.). Then, the PET-PDMS mask was removed from the PETG microfluidic device after sputtering and the device was connected to a printed circuit board (PCB) using copper wires and conductive silver glue (Fig. 1E/G). Three electrodes are then fabricated on the PETG microfluidic device. Different metal films can be selected, such as gold (Au), silver (Ag) and platinum (Pt). All these metal films need to use chromium (Cr) as an adhesion layer. As a proof of concept, all three electrodes are fabricated using Cr/Au film in this paper. The size of the device is shown in Fig. 1F/G.

2.3. Characterization of the gold film electrode (GFE)

The elemental composition and phase structures of the GFE were characterized using energy dispersive x-ray spectroscopy (EDS, Oxford Instruments Nano Analysis, USA) and X-ray Diffraction (XRD, Bruker AXS D8, USA). The morphologies of GFE was characterized by atomic force microscopy (AFM, Asylum Research, Santa Barbara, USA).

2.4. CV, DPV and EIS tests of the electrochemical sensor on the PETG microfluidic device

Cyclic voltammetry (CV), differential pulse voltammetry (DPV) and electrochemical impedance spectroscopy (EIS) were performed to demonstrate the performance of the electrochemical sensor on the PETG microfluidic device. All electrochemical measurements were carried out using an Autolab PGSTAT12 electrochemical workstation (Metrohm) in the presence of 5 mM $K_3[Fe(CN)_6]/K_4[Fe(CN)_6]$ as a redox probe in 1 M KCl. All the experiments were carried out at a Faraday cage.

2.5. Dopamine detection

The CV was performed between -0.2 V–0.6 V with a scan rate of 0.05 V/s in 0.1 M phosphate buffer solution containing DA and AA. Firstly, CV was carried out in 1 mM AA and 1 mM DA respectively. Then, the DA solutions with different concentrations of 1 mM, 5 mM, 10 mM were tested. Subsequently, DA solutions with different concentrations of 1 mM, 5 mM, 10 mM mixture with 10 mM AA was tested.

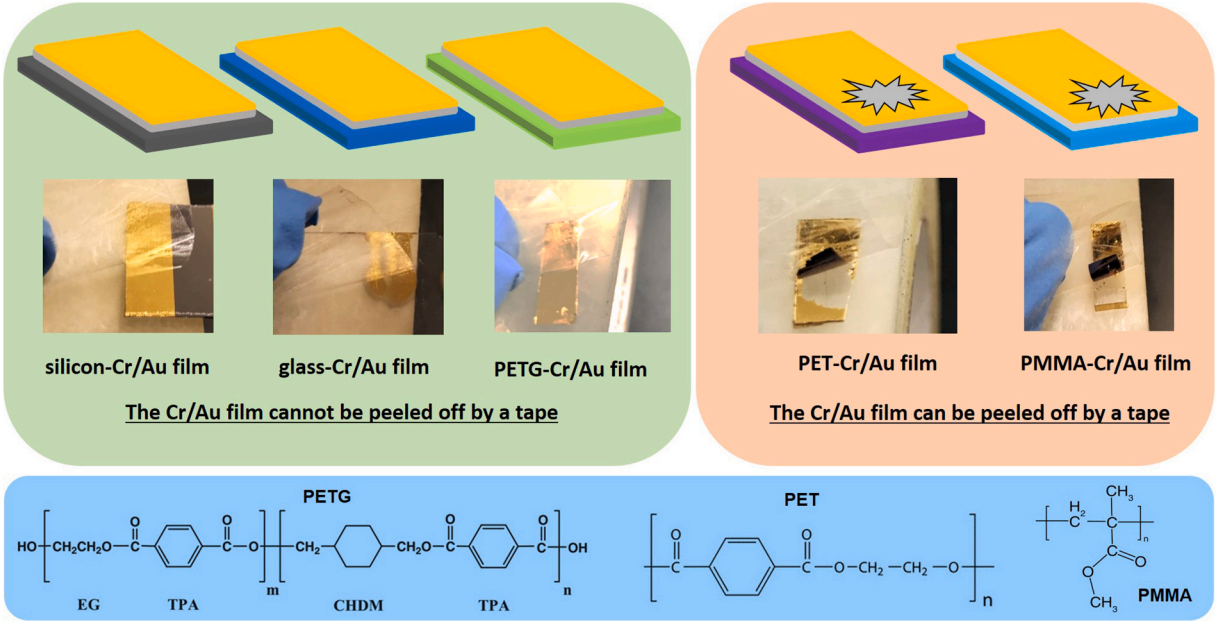

Fig. 2. Stability of Cr/Au film on silicon, glass, PETG, PET, and PMMA substrate using a common tape (Scotch, 3M) to peel the film and chemical structures of PETG, PET and PMMA. CHDM:1,4-cyclohexane dimethanol. EG: Ethylene glycol. TPA: Terephthalic acid. (For interpretation of the references to colour in this figure legend, the reader is referred to the Web version of this article.)

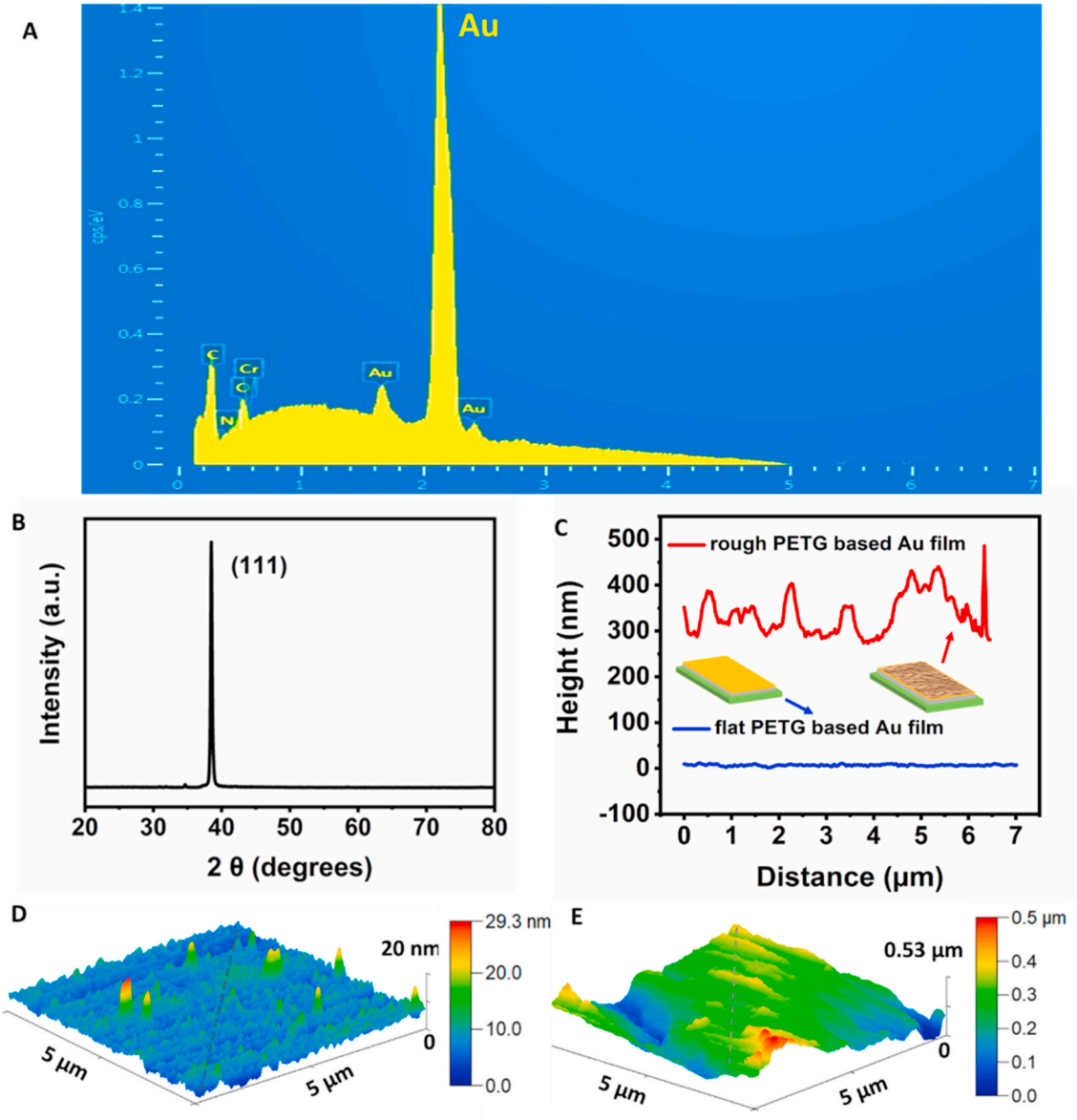

Fig. 3. (A) The EDS spectrum of the GFE on the PETG substrate with an accelerating voltage of 5.0 kV and probe current of medium-13. (B) XRD spectrum of bare GFE on the PETG substrate. (C) The roughness of the GFE on the processed PETG microfluidic device and a non-processed PETG substrate. (D) AFM image of GFE on non-processed PETG substrate. (E) AFM image of GFE on processed PETG microfluidic device.

3. Results and discussion

3.1. Design of PETG microfluidic device and choice of substrates

A novel methodology for the fabrication of electrochemical sensors on a polymer microfluidic device is developed. CNC machine was used for the automatic fabrication of multiple PETG microfluidic devices with microchannels in one step. To ensure the connectivity of the GFE, a slanted and smooth structure was designed to replace the vertical structure (Fig. 1H). Additionally, the design of the PETG microfluidic device allows one to use functional tape as a cover to fabricate the PETG-tape hybrid microfluidic device. Herein, hydrophilic tapes are used as covers. Complex sealing procedures such as thermal bonding and plasma processing are avoided. Different from the most reported "glass-PDMS" hybrid microfluidic device, the "PETG-tape" hybrid microfluidic device possesses the advantage of easy preparation (non-requirement of photolithography) and low cost.

Both CNC milling of the PETG platform and sputtering of patterned electrodes can be fabricated in batch. The CNC milling process is automatically controlled by a computer. As long as the design file is loaded to the computer and the PETG sheet is clamped, a large number of devices can be fabricated without any human interactions, rendering a batch fabrication process. A typical photo of such an automatic milling process is shown in Fig. 1A–C, where 20 devices were cut from the same piece of PETG. The sputtering step is also a batch process since multiple devices are sputtered at the same time without any additional cost of time or coating materials. Such batch fabrication processes help to increase the throughput of the device fabrication, decrease the cost of each device, and provide a potential for commercialization. Features of different methods for batch fabrication of electrochemical microfluidic devices are compared in Table 1.

Initially, the PMMA sheet was selected as the substrate for preparing the microfluidic device. However, it was found that the Cr/Au film cannot adhere to the PMMA substrate well. Especially when using tape as a cover, the tape can easily peel off the Cr/Au film sputtered on the PMMA substrate. To look for a suitable substrate, three other different

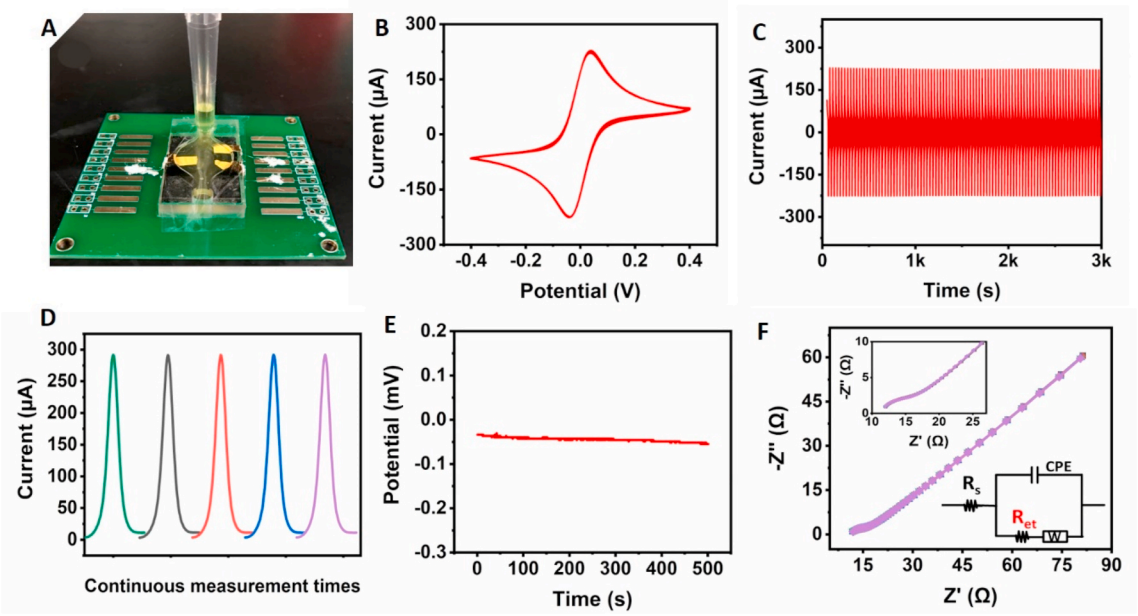

Fig. 4. (A) Picture of an assembled PETG microfluidic device; (B) 100 CV scans of an electrochemical sensor, with a scan rate of 0.05 V/s; (C) Plot of current to time in 3000 s; (D) Five DPV tests of the electrochemical sensor with a step of 50 mV, modulation amplitude of 25 mV, modulation time 0.05 s and interval time 0.5 s; (E) OCP of the electrochemical sensor with 500 s; (F) Five EIS tests and their Nyquist plots. All the tests are conducted with 1 M KCl containing 5 mM $K_3[Fe(CN)_6]/K_4$ [Fe $(CN)_6$] on the PETG microfluidic device.

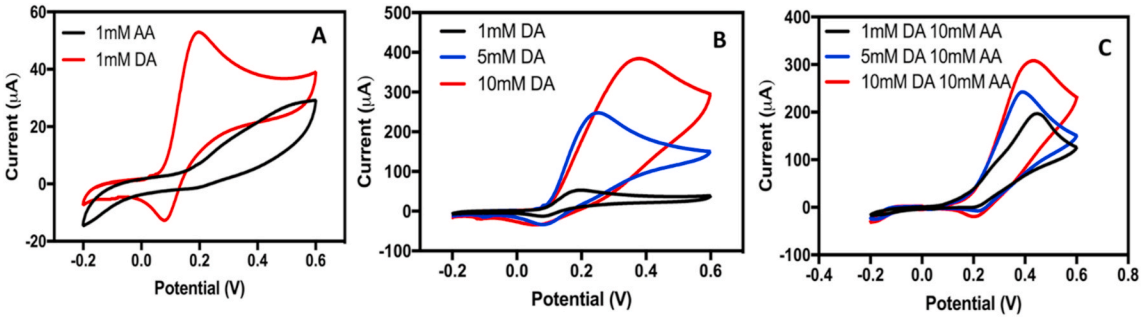

Fig. 5. CV plots recorded between -0.2 V–0.6 V by the electrochemical sensor on the PETG microfluidic device. (A) 1 mM AA and 1 mM DA, (B) Increasing concentration of DA from 1 mM–10 mM, (C) Increasing concentration of DA in presence of 10 mM AA.

polymer substrates including white PET (McMaster-Carr, 8597K92), transparent PET (Professional Plastics, SPETCL. 125RTM), transparent PETG (McMaster-Carr, 85815K16) are explored. The results show that the Cr/Au film has some adhesion to PET (transparent), but it is not robust. By comparison, the adhesion of Cr/Au to the PETG (transparent) was excellent. The tape peel-off tests were carried out on silicon-Cr/Au film, glass-Cr/Au film, PETG-Cr/Au film, PET-Cr/Au film, and PMMA-Cr/Au film (Fig. 2). It was demonstrated that the silicon-Cr/Au film, glass-Cr/Au film and PETG-Cr/Au film cannot be peeled off by tape. PET-Cr/Au film and PMMA-Cr/Au film can be peeled off by a tape. The electrochemical stability of PETG-Cr/Au film, PET-Cr/Au film, and PMMA-Cr/Au film are described in supplemental materials S2. The results proved excellent electrochemical stability of PETG-Cr/Au film. PETG is a type of low-temperature thermoplastic sheet/film with favorable thermoformability, machining performance, and chemical resistance. It is also a type of very cost-effective polymer substrate. Furthermore, PETG not only has noticeable toughness, enough stiffness to maintain the fluidic channel geometry, optical clarity for imaging, and high manufacturability but also is an environmentally friendly and healthy plastic resin (Kim et al., 2012). The results revealed that PETG is an excellent polymer substrate for developing plastic electrochemical devices, flexible electrochemical sensors and polymer microfluidic systems.

The chemical structure of PETG, PET and PMMA are shown in Fig. 2.

3.2. *Characterization of gold film electrode (GFE)*

The elemental composition and phase structures of the GFE were characterized using EDS and XRD. The EDS spectrum of the GFE is shown in Fig. 3A. The Au is the main elemental composition of GFE. As displayed in and XRD result (Fig. 3B), all the peaks can be indexed to the Au (111) crystal plane. The roughness of unprocessed PETG-based GFE and CNC-machined PETG-based GFE are presented in Fig. 3C. It is evident that the CNC-machined PETG-based GFE has a higher roughness. Our previous work showed that higher roughness can promote the Cr/Au film adherence to the polymer substrate and enhance the sensitivity of the electrochemical sensor (Cui et al., 2020a). Hence, CNC-machined PETG-based GFE on the microfluidic device can make the GFE more stable and the electrochemical sensor more robust. The morphologies of the GFE on unprocessed PETG and CNC-machined PETG were shown in Fig. 3D/E respectively.

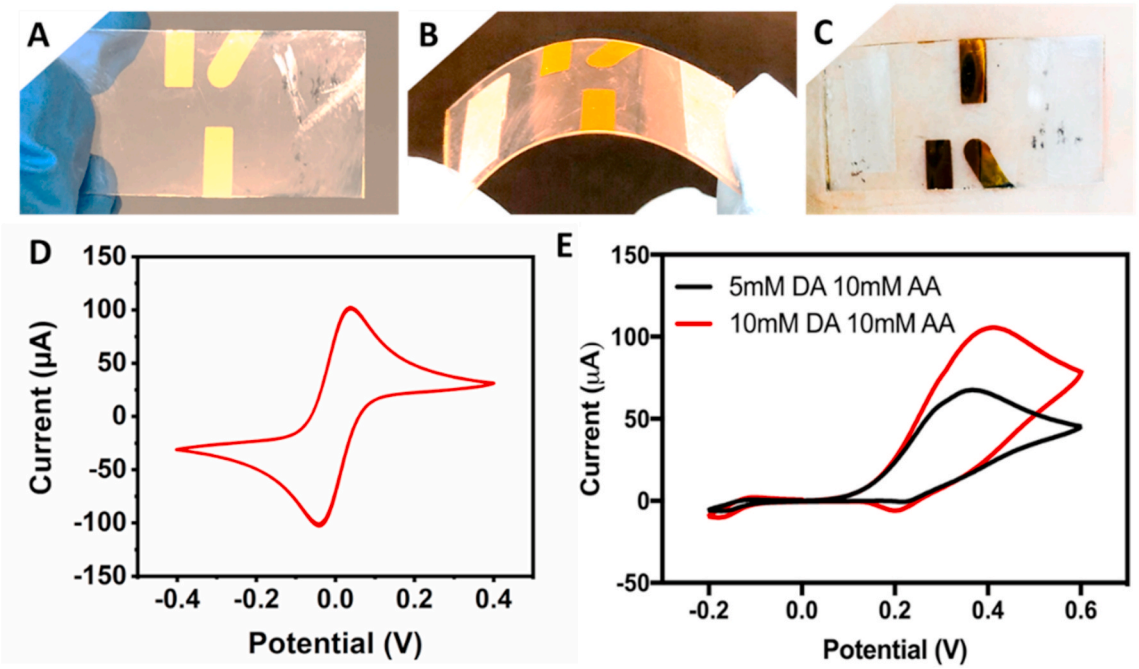

Fig. 6. Images of the flexible electrochemical sensor on the soft PETG film. Normal view (A), bending view (B), and fitted in the arm view (C). (D) 100 CV scans of an electrochemical sensor, with a scan rate of 0.05 V/s in1 M KCl containing 5 mM $K_3[Fe(CN)_6]/K_4$ $[Fe(CN)_6]$; (E) CV plots in PBS solution (pH = 7.4) containing a mixture of 5 mM DA and 10 mM AA (black curve), and containing a mixture of 10 mM DA and 10 mM AA (red curve). (For interpretation of the references to colour in this figure legend, the reader is referred to the Web version of this article.)

3.3. Electrochemical performance of the sensor on the PETG microfluidic device

A real image of the PETG microfluidic device is shown in Fig. 4A. CV, DPV and EIS detection techniques were applied to characterize the GFE on the PETG microfluidic device. The stability of the electrode was evaluated by CV with 100 scans (Fig. 4B) in 1 M KCl*containing* 5 mM $K_3[Fe(CN)_6]/K_4[Fe(CN)_6]$. The current-time curve was recorded in Fig. 4C within 3000 s. The results showed that the stability of GFE was good enough for an electrochemical sensor. Five groups of DPV of the same device was continuously measured. The DPV plots were presented in Fig. 4D and the value of peak current was 291.6 ± 0.40 mA with the coefficient of variation (CV) of 0.14%. The results reveal that the GFE exhibited good electrochemical stability to perform the DPV test.

Open circuit potential (OCP) is important to conduct the EIS test (Ramanathan et al., 2016). OCP was recorded within 500 s as shown in Fig. 4F and it showed no obvious potential shift. The OCP of the electrochemical microfluidic device was -0.04470 ± 0.0047 mV with a CV of 10.31%. It showed a relatively good stability of the device, and especially good stability of the reference electrode. Subsequently, five groups of EIS tests of the same device were measured with a frequency range of $1–10^5$ Hz, the amplitude of 10 mV to OCP. The Nyquist plots presented in Fig. 4F was analyzed by the Randles equivalent circuit (Cui et al., 2018). The electron transfer resistance (R_{et}) was 3.870 ± 0.0098 Ω with a CV of 0.25% which revealed good EIS response of the device.

3.4. Dopamine test in the microfluidic device

DA is one of the most important neurotransmitters in the mammalian central nervous system, as low levels of dopamine may bring about Parkinson's disease (Kim et al., 2002). Dopamine is also a type of catecholamine that can be detected electrochemically on a gold electrode. Ascorbic acid (AA) is a common antioxidant coexisting with dopamine in biologic samples and oxidized at the almost same potential region as dopamine. It was reported that the addition of ascorbic acid to dopamine will cause a Δ0.2 V positive shift of oxidation peak on the bare gold electrode (Yang et al., 2014).

Considering the physiological environment, the PBS buffer solution at a pH of 7.4 was chosen as the supporting electrolyte for the experiments. CV of dopamine and ascorbic acid was shown in Fig. 5. For dopamine, a pair of redox peaks occurred at 0.2 V and 0.08 V (Fig. 5A), corresponding to the two electrons oxidation of DA to o-dopaminoquinone and subsequent reduction of o-dopaminoquinone to DA, respectively (Łuczak, 2008). In contrast, there is no obvious oxidation peak and reduction peak for ascorbic acid. This demonstrates that the bare GFE on the PETG microfluidic device is electroactive towards the oxidation of dopamine.

To test the analytical electrochemical performance toward dopamine, CV was obtained at dopamine concentration of 1 mM, 5 mM and 10 mM. As shown in Fig. 5B, peak currents of dopamine oxidation increased from 52 μA to 382 μA with the increased concentration of dopamine from 1 mM to 10 mM. This result revealed the good analytical electrochemical performance of the electrode toward dopamine.

The CV responses of the mixture solution of dopamine and ascorbic acid are shown in Fig. 5C. After adding ascorbic acid into dopamine solution, one oxidation peak at 0.4 V occurred. Compared to the oxidation peak that occurred at 0.2 V with only dopamine, a positive shift of 0.2 V was observed. The oxidation peak shift matched with studies of dopamine and ascorbic acid on the bare gold electrode published before (Yang et al., 2014). In the meantime, we show that with the existence of ascorbic acid, the peak current still increased with increasing dopamine concentration. This demonstrates that the electrode maintained the analytical electrochemical performance in presence of interference species.

3.5. Flexible electrochemical sensor on the PETG film

Nowadays, flexible electrochemical sensors are the most popular and draw great attention to health monitoring (Ferreira et al., 2019; Xuan et al., 2018; Zhang et al., 2019). Thanks to the good adhesion of PETG substrate and Cr/Au film, a flexible electrochemical sensor with three electrodes are fabricated on PETG film (Fig. 6 A/B/C). The detailed

protocol for the preparation of flexible electrochemical sensors is presented in supplemental materials S3. The stability of the flexible electrochemical sensor was evaluated by CV with 100 scans (Fig. 6D) in 1 M KCl containing 5 mM $K_3[Fe(CN)_6]/K_4[Fe(CN)_6]$. The results show excellent stability. It proves that the PETG is a novel polymer substrate for the fabrication of flexible electrochemical sensors.

The CV responses of the mixture solution of DA and AA were recorded at the flexible Au electrode (Fig. 6E). The oxidation peak at about 0.4 V occurred and oxidation peak current increased with increasing dopamine concentration, which is consistent with the CV on bare GFE on PETG-based substrate. This demonstrated the electroactive performance of the flexible Au electrode toward dopamine as well.

4. Conclusions

In this paper, we demonstrate electrochemical microfluidic devices and flexible electrochemical sensors based on the PETG substrate. PMMA, PET, and PETG are explored as a substrate for fabricating the electrochemical biosensor. Among them, the PETG exhibits robust adhesion to the Cr/Au film comparable to that of silicon and glass substrates. Our novel developed methodology for the fabrication of the electrochemical microfluidic devices leads to a high roughness of the GFE, which can enhance the stability and sensitivity of the electrochemical sensors. In the 1 M KCl containing 5 mM $K_3[Fe(CN)_6]/K_4[Fe(CN)_6]$, the peak current of DPV test was 291.6 ± 0.40 mA with the coefficient of variation (CV) of 0.14%, the OCP was -0.04470 ± 0.0047 mV with the CV of 10.31% and the R_{et} was 3.870 ± 0.0098 Ω with the CV of 0.25%. The results showed excellent electrochemical performance for both electrochemical microfluidic devices and flexible electrochemical sensors based on the PETG substrate. Meanwhile, both of them show good performance for the detection of DA.

CRediT authorship contribution statement

Feiyun Cui: Conceptualization, Writing - original draft, Methodology. **Hamed Jafarishad:** Writing - original draft. **Zhiru Zhou:** Writing - original draft. **Jiazhang Chen:** AFM test and analysis. **Jiahui Shao:** Conceptualization. **Qi Wen:** AFM test and analysis. **Yuxiang Liu:** Conceptualization, Writing - review & editing, Supervision, Funding acquisition. **H. Susan Zhou:** Conceptualization, Writing - review & editing, Supervision, Funding acquisition.

Declaration of competing interest

The authors declare that they have no known competing financial interests or personal relationships that could have appeared to influence the work reported in this paper.

Acknowledgments

This work was supported by the National Science Foundation (CBET-1805514).

Appendix A. Supplementary data

Supplementary data to this article can be found online at https://doi.org/10.1016/j.bios.2020.112521.

References

Bariya, M., Shahpar, Z., Park, H., Sun, J., Jung, Y., Gao, W., Nyein, H.Y.Y., Liaw, T.S., Tai, L.-C., Ngo, Q.P., 2018. Roll-to-roll gravure printed electrochemical sensors for wearable and medical devices. ACS Nano 12 (7), 6978–6987.

Cagnani, G.R., Ibáñez-Redín, G., Tirich, B., Gonçalves, D., Balogh, D.T., Oliveira Jr., O. N., 2020. Fully-printed electrochemical sensors made with flexible screen-printed electrodes modified by roll-to-roll slot-die coating. Biosens. Bioelectron. 112428.

Carvajal, S., Fera, S.N., Jones, A.L., Baldo, T.A., Mosa, I.M., Rusling, J.F., Krause, C.E., 2018. Disposable inkjet-printed electrochemical platform for detection of clinically relevant HER-2 breast cancer biomarker. Biosens. Bioelectron. 104, 158–162.

Choi, C.J., Cunningham, B.T., 2006. Single-step fabrication and characterization of photonic crystal biosensors with polymer microfluidic channels. Lab Chip 6 (10), 1373–1380.

Cincotto, F.H., Fava, E.L., Moraes, F.C., Fatibello-Filho, O., Faria, R.C., 2019. A new disposable microfluidic electrochemical paper-based device for the simultaneous determination of clinical biomarkers. Talanta 195, 62–68.

Cui, F., Xu, Y., Wang, R., Liu, H., Chen, L., Zhang, Q., Mu, X., 2018. Label-free impedimetric glycan biosensor for quantitative evaluation interactions between pathogenic bacteria and mannose. Biosens. Bioelectron. 103, 94–98.

Cui, F., Zhou, Z., Zhou, H.S., 2019. Measurement and analysis of cancer biomarkers based on electrochemical biosensors. J. Electrochem. Soc. 167 (3), 037525.

Cui, F., Zhou, Z., Feng, H., Zhou, H.S., 2020a. Disposable polyurethane nanospiked gold electrode-based label-free electrochemical immunosensor for Clostridium difficile. ACS Applied Nano Materials 3 (1), 357–363.

Cui, F., Zhou, Z., Zhou, H.S., 2020b. Molecularly imprinted polymers and surface imprinted polymers based electrochemical biosensor for infectious diseases. Sensors 20 (4), 996.

da Silva, E.N.T., Ferreira, V.S., Lucca, B.G., 2019. Rapid and inexpensive method for the simple fabrication of PDMS-based electrochemical sensors for detection in microfluidic devices. Electrophoresis 40 (9), 1322–1330.

Fava, E.L., Silva, T.A., Prado, T.M.d., Moraes, F.C.d., Faria, R.C., Fatibello-Filho, O., 2019. Electrochemical paper-based microfluidic device for high throughput multiplexed analysis. Talanta 203, 280–286.

Fernández-la-Villa, A., Pozo-Ayuso, D.F., Castaño-Álvarez, M., 2019. Microfluidics and electrochemistry: an emerging tandem for next-generation analytical microsystems. Current Opinion in Electrochemistry 15, 175–185.

Ferreira, P.C., Ataide, V.N., Chagas, C.L.S., Angnes, L., Coltro, W.K.T., Paixão, T.R.L.C., de Araujo, W.R., 2019. Wearable electrochemical sensors for forensic and clinical applications. Trac. Trends Anal. Chem. 119, 115622.

Jang, H., Pawate, A.S., Bhargava, R., Kenis, P.J., 2019. Polymeric microfluidic continuous flow mixer combined with hyperspectral FT-IR imaging for studying rapid biomolecular events. Lab Chip 19 (15), 2598–2609.

Kim, J.H., Auerbach, J.M., Rodríguez-Gómez, J.A., Velasco, I., Gavin, D., Lumelsky, N., Lee, S.H., Nguyen, J., Sánchez-Pernaute, R., Bankiewicz, K., McKay, R., 2002. Dopamine neurons derived from embryonic stem cells function in an animal model of Parkinson's disease. Nature 418 (6893), 50–56.

Kim, I.G., Hong, S.Y., Park, B.O., Choi, H.J., Lee, J.H., 2012. Polyphenylene ether/glycol modified polyethylene terephthalate blends and their physical characteristics. J. Macromol. Sci., Part B 51 (4), 798–806.

Lakey, A., Ali, Z., Scott, S.M., Chebil, S., Korri-Youssoufi, H., Hunor, S., Ohlander, A., Kuphal, M., Marti, J.S., 2019. Impedimetric array in polymer microfluidic cartridge for low cost point-of-care diagnostics. Biosens. Bioelectron. 129, 147–154.

Lee, K., Yoon, T., Yang, H.-s., Cha, S., Cheon, Y.-P., Kashefi-Kheyrabadi, L., Jung, H.-I., 2020. All-in-one platform for salivary cotinine detection integrated with a microfluidic channel and an electrochemical biosensor. Lab Chip 20, 320–331.

Liu, J., Qin, J., Li, J., Li, D., Xu, Z., Zhang, X., Du, L., Liu, C., 2013. Monolithic integration of three-material microelectrodes for electrochemical detection on PMMA substrates. Electrochem. Commun. 31, 20–23.

Liu, L., Xu, Y., Cui, F., Xia, Y., Chen, L., Mou, X., Lv, J., 2018. Monitoring of bacteria biofilms forming process by in-situ impedimetric biosensor chip. Biosens. Bioelectron. 112, 86–92.

Nikoleli, G.-P., Siontorou, C.G., Nikolelis, D.P., Bratakou, S., Karapetis, S., Tzamtzis, N., 2018. Biosensors based on microfluidic devices lab-on-a-chip and microfluidic technology. Nanotechnology and Biosensors 375–394 (Elsevier).

Oliveira, G.C.M.d., Carvalho, J.H.d.S., Brazaca, L.C., Vieira, N.C.S., Janegitz, B.C., 2020. Flexible platinum electrodes as electrochemical sensor and immunosensor for Parkinson's disease biomarkers. Biosens. Bioelectron. 152, 112016.

Ramanathan, M., Patil, M., Epur, R., Yun, Y., Shanov, V., Schulz, M., Heineman, W.R., Datta, M.K., Kumta, P.N., 2016. Gold-coated carbon nanotube electrode arrays: immunosensors for impedimetric detection of bone biomarkers. Biosens. Bioelectron. 77, 580–588.

Ren, Y., Ray, S., Liu, Y., 2019. Reconfigurable acrylic-tape hybrid microfluidics. Sci. Rep. 9 (1), 1–10.

Rocha, R.G., Cardoso, R.M., Zambiazi, P.J., Castro, S.V.F., Ferraz, T.V.B., de, O., Aparecido, G., Bonacin, J.A., Munoz, R.A.A., Richter, E.M., 2020. Production of 3D-printed disposable electrochemical sensors for glucose detection using a conductive filament modified with nickel microparticles. Anal. Chim. Acta 1132, 1–9.

Rodrigues, R.O., Lima, R., Gomes, H.T., Silva, A.M., 2015. Polymer microfluidic devices: an overview of fabrication methods. U. Porto Journal of Engineering 1 (1), 67–79.

Shi, H., Zhu, F., Zhou, X., Li, H., Yang, F., Zhang, X., Liu, J., 2019. Large scale fabrication of disposable carbon cloth electrochemical sensors for simultaneous determination of heavy metal ion. J. Electroanal. Chem. 840, 328–337.

Tsao, C.-W., 2016. Polymer microfluidics: simple, low-cost fabrication process bridging academic lab research to commercialized production. Micromachines 7 (12), 225.

Wang, P., Wang, M., Zhou, F., Yang, G., Qu, L., Miao, X., 2017a. Development of a paper-based, inexpensive, and disposable electrochemical sensing platform for nitrite detection. Electrochem. Commun. 81, 74–78.

Wang, R., Xu, Y., Liu, H., Peng, J., Irudayaraj, J., Cui, F., 2017b. An integrated microsystem with dielectrophoresis enrichment and impedance detection for detection of Escherichia coli. Biomed. Microdevices 19 (2), 34.

Wang, Y., Luo, J., Liu, J., Sun, S., Xiong, Y., Ma, Y., Yan, S., Yang, Y., Yin, H., Cai, X., 2019. Label-free microfluidic paper-based electrochemical aptasensor for

ultrasensitive and simultaneous multiplexed detection of cancer biomarkers. Biosens. Bioelectron. 136, 84–90.
Xuan, X., Yoon, H.S., Park, J.Y., 2018. A wearable electrochemical glucose sensor based on simple and low-cost fabrication supported micro-patterned reduced graphene oxide nanocomposite electrode on flexible substrate. Biosens. Bioelectron. 109, 75–82.
Yang, L., Liu, D., Huang, J., You, T., 2014. Simultaneous determination of dopamine, ascorbic acid and uric acid at electrochemically reduced graphene oxide modified electrode. Sensor. Actuator. B Chem. 193, 166–172.
Yang, J., Hu, Y., Li, Y., 2019. Molecularly imprinted polymer-decorated signal on-off ratiometric electrochemical sensor for selective and robust dopamine detection. Biosens. Bioelectron. 135, 224–230.
Zhang, Z., Azizi, M., Lee, M., Davidowsky, P., Lawrence, P., Abbaspourrad, A., 2019. A versatile, cost-effective, and flexible wearable biosensor for in situ and ex situ sweat analysis, and personalized nutrition assessment. Lab Chip 19 (20), 3448–3460.
Łuczak, T., 2008. Preparation and characterization of the dopamine film electrochemically deposited on a gold template and its applications for dopamine sensing in aqueous solution. Electrochim. Acta 53 (19), 5725–5731.